Electrochemistry Communications 170 (2025) 107855

Contents lists available at ScienceDirect

Electrochemistry Communications

journal homepage: www.elsevier.com/locate/elecom

Short Communication

TiO_2 nanotubes grown on Ti and Ti6Al4V alloy spheres by bipolar anodization

Marcela Sepúlveda [a,b,*], Hanna Sopha [a,b], Veronika Cicmancova [a], Ludek Hromadko [a,b], Jan M. Macak [a,b,*]

[a] Center of Materials and Nanotechnologies, Faculty of Chemical Technology, University of Pardubice, Nam. Cs. Legii 565, 53002 Pardubice, Czech Republic
[b] Central European Institute of Technology, Brno University of Technology, Purkynova 123, 612 00 Brno, Czech Republic

ARTICLE INFO

Keywords:
Bipolar electrochemistry
TiO_2 nanotube layers
Ti spheres
Ti6Al4V alloy
Ti6Al4V spheres

ABSTRACT

In this work, the anodization of spheres of Ti and Ti6Al4V alloy (TiAlV) in glycerol-based electrolytes using bipolar electrochemistry is shown for the first time. TiO_2 nanotube (TNT) layers were found over the entire surface area of the Ti and TiAlV spheres using a square wave potential of ±60 V and ±65 V with 5.56×10^{-4} Hz. The TNTs' inner diameter on the extremities of the Ti spheres was ~63 nm and ~78 nm, for ±60 V and ±65 V, respectively. The inner diameter of the TNTs fabricated on the TiAlV spheres was ~36 nm and ~43 nm for ±60 V and ±65 V, respectively. The effect of the alloying elements of the TiAlV spheres on the TNT layers was also investigated. To estimate the effective potential on the spheres contributing to the TNT layer formation, also the conventional anodization was performed on flat Ti and TiAlV foils for comparison. It was found that the effective potential reached on the extremities of the Ti and TiAlV spheres near the feeder electrodes was only 29 % and 16 % of the applied potential, respectively.

1. Introduction

Bipolar electrochemistry has opened new avenues of research in the field of electrochemistry. Unlike traditional electrochemical methods, bipolar electrochemistry involves inducing redox reactions on a conductive material, known as a bipolar electrode, which is placed wirelessly between feeder electrodes. This technique has been studied since the 1960s [1–3]. However, it was only in 2014, when bipolar electrochemistry was introduced as a technique for the growth of TiO_2 nanotube (TNT) layers on Ti foils in open anodization cells [4,5]. Recently, Asoh et al [6,7], showed the possibility of using bipolar electrochemistry for the indirect oxidation of Al under an AC electric field.

In a bipolar electrochemical setup, the metal substrate (such as aluminium [8], titanium [9], niobium [10], etc.) functions as a bipolar electrode (BPE), placed between two feeder electrodes immersed in a suitable electrolyte. The electrical potential is applied to the feeder electrodes, while the BPE is not directly connected to the potentiostat. Instead, it is polarized by the electric field generated between the feeder electrodes [11,12]. As a result, the side of the BPE facing the feeder cathode acts as the anodic pole, where oxidation reactions occur, while the opposite side, facing the feeder anode, acts as a cathodic pole leading to reduction reactions. However, since the redox reaction occurs on a wireless BPE, the voltage associated with the chemical reactions cannot be directly measured, as in conventional (wired) methods. To address this challenge, some studies have focused on visualizing the potentials and potential distributions along the surfaces of BPEs [8,13]. For instance, Asoh et al [10,13,14], employed an electrochemical characterization method, specifically re-anodization, on alumina compact layer films, to estimate the effective potential during bipolar anodization.

Anodizing complex 3D Ti-based structures to modify them with TNT layers is a challenging task, as the large surface area increases the risk of dielectric breakdown [15,16]. Additionally, for complete anodization, the entire 3D structure must be fully immersed into the electrolyte while maintaining a connection to the potentiostat. This is nearly impossible for solid structures like spheres. To overcome these challenges, we recently demonstrated the feasibility of bipolar anodization of different 3D structures namely as Ti spheres, and 3D-printed Ti meshes using ethylene glycol-based electrolytes [17–19].

* Corresponding authors at: Center of Materials and Nanotechnologies, Faculty of Chemical Technology, University of Pardubice, Nam. Cs. Legii 565, 53002 Pardubice, Czech Republic.
E-mail addresses: lise1589@upce.cz (M. Sepúlveda), Jan.Macak@upce.cz (J.M. Macak).

https://doi.org/10.1016/j.elecom.2024.107855
Received 25 October 2024; Received in revised form 9 December 2024; Accepted 13 December 2024
Available online 14 December 2024

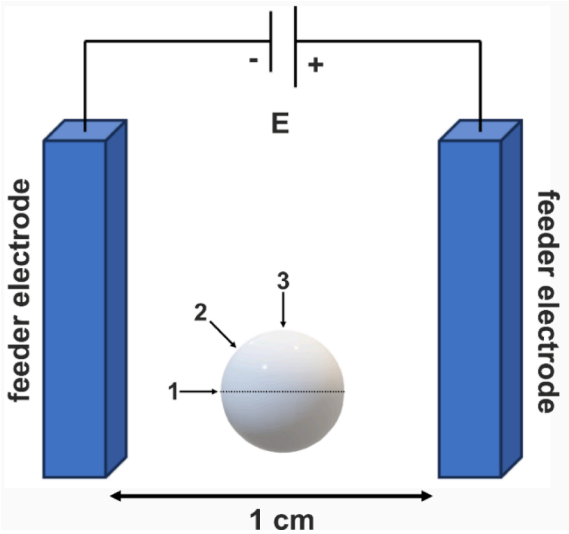

Fig. 1. Schematic of the Ti and TiAlV spheres during bipolar anodization. The arrows indicate the spots where the SEM top-view images were taken.

In this communication, we systematically investigate, for the first time, the anodization of small Ti6Al4V (TiAlV) spheres (2 mm in diameter) using bipolar electrochemistry. Ti spheres (3 mm in diameter) were also anodized for comparison. Conformal anodization across the entire surface area was achieved by applying a square-wave voltage in glycerol-based electrolytes. Taking a similar approach as Asoh et al. [13,14], Ti and TiAlV foils were also anodized at different potentials using conventional anodization, and the inner diameter was compared with those obtained via bipolar electrochemistry on the spheres to estimate the effective potential reached on the sphere surfaces.

2. Experimental

The bipolar anodization setup is shown in Fig. 1. It consisted of two Pt electrodes placed 1 cm apart, used as feeder electrodes, and connected to a high-voltage potentiostat (PGU-200V; Elektroniklabor GmbH). Ti spheres (Goodfellow, 99.6+%, 3 mm diameter), and TiAlV spheres (Goodfellow, 2 mm diameter) were cleaned by sonication in isopropanol and acetone for 2 min each. After that, the spheres were positioned in the center between the two feeder electrodes (see Fig. 1) on adhesive tape to prevent random movement during anodization. Anodization was performed in 200 ml of a glycerol-based electrolyte containing 270 mM NH_4F, 50 vol% H_2O, and 50 vol% glycerol. A rectangular square wave potential with an amplitude of ±60 V and ±65 V and a frequency of 5.56×10^{-4} Hz (meaning the potential was changed every 30 min) was applied. The total anodization time was 180 min. The electrolyte was cooled to 5 °C before and during anodization using a thermostat and a cooling coil to maintain a stable temperature. After anodization, the Ti and TiAlV spheres were sonicated in isopropanol for 5 min and then air-dried. Conventional anodization was performed on Ti and TiAlV foils at different potentials between +5 V and +25 V for 180 min using the same glycerol-based electrolyte as for the spheres. The inner diameter of the TNTs obtained at different potentials for both types of foils was evaluated and compared to the inner diameters of the TNTs obtained on both types of spheres.

The morphological features of the anodized Ti and TiAlV spheres were characterized using a field-emission scanning electron microscope (FE-SEM, JEOL, JSM 7500F). SEM top-view images were taken at three specific locations: near the extremities – i.e. closest point to the feeder electrodes (1), on the site, 45° parallel to feeder electrodes (2), and at the top of the sphere, parallel to the feeder electrodes (3) as shown in Fig. 1.

3. Results and discussion

Fig. 2 shows a set of top-view SEM images of the Ti spheres, acting as BPE, anodized at two different voltages – ±60 V and ±65 V – applied between the feeder electrodes, using a frequency of 5.56×10^{-4} Hz. Fig. 2 a), b), and c) show the TNT layers obtained after anodization at ±60 V on spots 1, 2, and 3, respectively, and Fig. 2 d), e) and f) depict the TNT layers grown at ±65 V on spots 1, 2, and 3, respectively. As one can see, TNT layers were found on all the spots of the Ti spheres. Upon detailed measurements, at the extremities of the Ti spheres facing the feeder electrodes (i.e., spot 1), the average inner diameter of the TNTs was ~63 nm and ~78 nm for ±60 V and ±65 V, respectively. In the positions between the extremities and the top of the spheres (spot 2), the TNTs inner diameter was ~46 nm and ~45 nm, respectively. On the top of the spheres (spot 3), the inner diameter of the TNTs was ~16 nm and ~19 nm, respectively. This phenomenon can be explained by the principles of bipolar electrochemistry, which are detailed in the literature [4,11,20]. In short, the applied potential decreases gradually across the electrolyte solution between the feeder electrodes. As a result, the polarization potential on the spheres also decreases along its length. The extremities of the spheres experience the highest polarization potential, which diminishes toward the center of the spheres. Consequently, the inner diameter and thickness of the TNT layers vary along the sphere [4]. In spot 3, TNT layers were found, even though the polarization potential around this position – according to the principles of bipolar electrochemistry – should be zero or very close to zero. Similar observations though can be found in the literature. For example, Loget et al. demonstrated that a gold bead could be half-coated with polypyrrole following wireless anodization [21,22]. Similarly, Asoh et al. reported that the zero-potential position was not at the center of the sample, resulting in an anodic reaction area that was significantly larger than expected, accounting for approximately 90 % of the bipolar electrode [8]. Furthermore, Wei et al. observed that TiO_2 nanotubes with a size gradient covered a substantial portion (approximately 75 %) of a Ti BPE during DC bipolar anodization [23]. These studies consistently indicate that the cathodic reaction (e.g., hydrogen evolution) is confined to a minimal region at the rightmost extremity (<25 %), which is closest to the feeder anode. In conclusion, the oxidized area becomes much larger than the region acting as a local cathode due to the temporal change in the passivation region on the Ti BPE [23,24].

Fig. 3 shows a set of the SEM top-view images of TiAlV spheres anodized at ±60 V and ±65 V. As with the Ti spheres, at the extremities of the spheres facing the feeder electrodes (spot 1) the TNTs fabricated on the TiAlV spheres had the largest average inner diameter of approximately ~36 nm, and ~43 nm for ±60 V and ±65 V, respectively. In the regions between the extremities and the top of the spheres (spot 2), the TNTs inner diameter was around ~30 nm and ~36 nm, respectively, while at the top of the spheres (spot 3), the inner diameters of the TNTs measured approximately ~17 nm and ~21 nm, respectively. The difference in the inner TNT diameters measured on Ti and TiAlV spheres is discussed below.

A square-wave potential was used to anodize the entire surface of the Ti and TiAlV spheres, as by applying a direct potential only the side of the spheres facing the feeder cathode can be oxidized while on the other side, a reduction reaction takes place (i.e. the reduction of H^+ to H_2). As a result, the tubes show a black appearance (due to the creation of Ti^{3+} states). There is hydrogen evolution as well, which stems from the negative applied voltage and contribution to the overall reduction process. By applying a square-wave potential, however, both sides of the spheres can be anodized after each other.

Several anodization potentials were studied from ±30 V up to ±70 V (not shown here). In the case of low applied potentials from ±30 V up to ±50 V, only porous TiO_2 layers were formed on the Ti and TiAlV spheres, while for high potentials of ±70 V no TNT layers were found anywhere on the spheres, or the TNT layers were destroyed. The reason for this is likely the strong H_2 evolution, caused by the high current

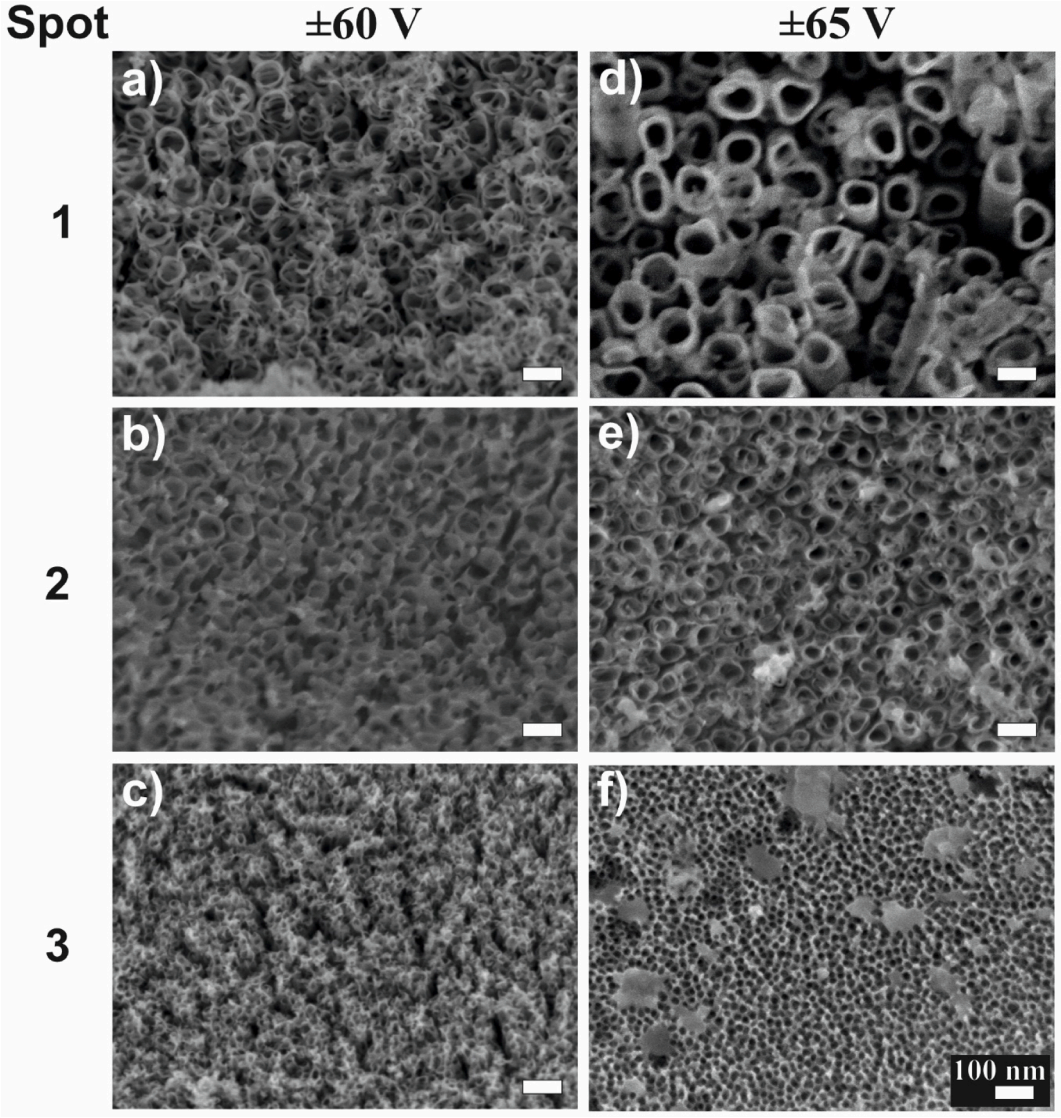

Fig. 2. SEM top-view images of TNT layers on Ti spheres with a diameter of 3 mm obtained after 180 min at a frequency of 5.56×10^{-4} Hz with an amplitude of ±60 V at spots 1, 2, and 3 (a–c), respectively, and with an amplitude of ±65 V at spots 1, 2, and 3 (d–f).

during the bipolar anodization, which destroys the previously produced TNT layers [18].

Since the potential distribution cannot be measured directly on the Ti and TiAlV spheres, a set of experiments was carried out using conventional anodization of flat Ti and TiAlV foils at different potentials (from +5 V up to +25 V). This potential range was selected as (i) the effective potential on the surface of the sphere is lower than the potential applied between the feeder electrodes during bipolar anodization, and (ii) our previous work [25] revealed that the average inner diameter of the TNTs measured on the spheres (see Figs. 2 and 3) corresponds to an effective potential within this range. The inner diameter of the TNTs obtained on the foils was measured and compared to the values obtained for the spheres anodized using bipolar anodization to understand the effective potential and its distribution on the BPE. Figs. S1 and S2 show the SEM top-view images of the TNT layers obtained on the Ti and TiAlV foils. Fig. 4 shows the dependence of the inner TNT diameter on the applied potential for the Ti and TiAlV foils using conventional anodization. As expected, the TNT diameter increases linearly with the applied potential for both kinds of foils [26,27].

As one can see, the inner diameter of the TNTs is overall smaller on the TiAlV foils than on the Ti foils. This is due to the aluminium and vanadium elements present in the TiAlV, which can affect the morphology of the TiO_2 nanotube layers [28]. In the TiAlV, aluminium stabilizes the α-phase, and vanadium stabilizes the β-phase. During anodization, the α and β phases exhibit different dissolution rates, leading to variations in the thickness and inner diameter of the TNT layers. The β-phase, enriched in vanadium, forms thinner nanotube layers due to its higher dissolution rate compared to the α-phase [28,29].

Due to the linear relationship between the inner TNT diameter and the applied potential, the effective potential on the Ti and TiAlV spheres can be calculated. In the case of spot 1 in Fig. 2, the inner nanotube diameter was ~63 nm and ~78 nm for the Ti spheres anodized at ±60 V and ±65 V which corresponds according to Fig. 4. a) an effective potential of ~16 V and ~19 V. This value is ~26 % and ~29 % of the potential applied to the feeder electrodes. In the case of TiAlV spheres, the values of the TNT layers' inner diameters on spot 1 were ~36 nm and ~43 nm, corresponding to an effective applied potential of ~10 V and ~12.5 V (Fig. 4. b), which is ~16 % and ~19 % of the applied potential. Thus, the anodization process of Ti and TiAlV spheres lead to quantitative differences indicating that a larger diameter of nanotubes and a higher effective potential is reached on Ti spheres compared to TiAlV spheres. The alloy's composition with vanadium and aluminium plays a significant role in these differences, resulting in smaller nanotube diameters. The effective applied potential difference for the TiAlV

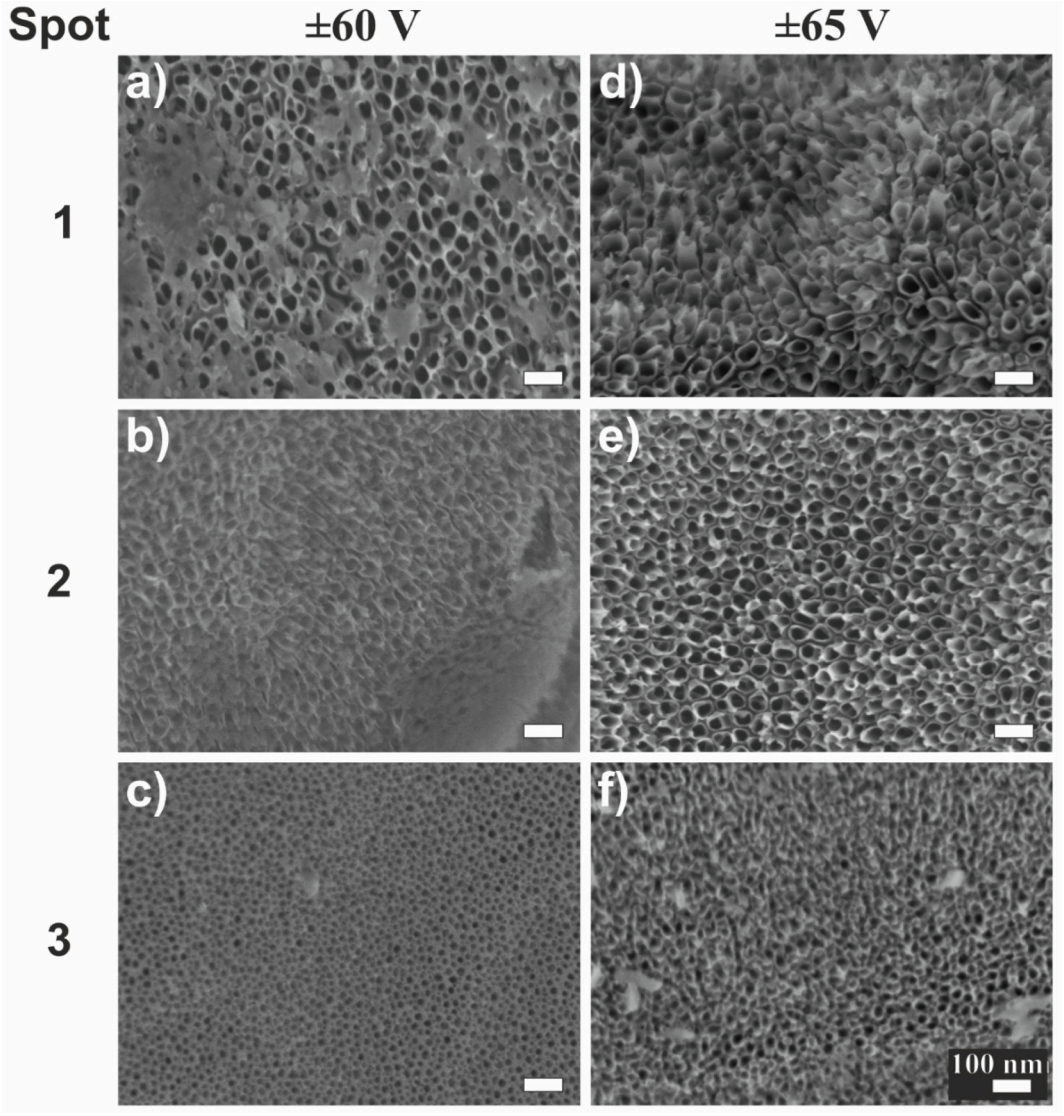

Fig. 3. SEM top-view images of TNT layers on TiAlV spheres with a diameter of 2 mm obtained after 180 min at a frequency of 5.56×10^{-4} Hz with an amplitude of ±60 V at spots 1, 2, and 3 (a–c), respectively, and with an amplitude of ±65 V at spots 1, 2, and 3 (d–f). Note: SEM images shows only α-phase regions of the alloy.

spheres is more evident than for Ti spheres, this can be attributed to the size of the TiAlV spheres, which are smaller (2 mm) than the Ti spheres (3 mm). As a result of the different sphere sizes, the distance between the extremities of the spheres and the feeder electrodes varies for both kinds of spheres, as the distance between the feeder electrodes is constant (1 cm). This results in a distance of 3.5 mm and 4 mm for the Ti and the TiAlV spheres, respectively, between the feeder electrodes and the extremities of the spheres. Therefore, the potentials reaching the TiAlV spheres are smaller. The results of the effective potential differ from those reported by Asoh et al [8,10] on aluminium sheets. In that case, the shape of the BPE was rectangular with different sizes and the distance between the BPE and the feeder electrodes was different than in our study, resulting in different effective potentials at the BPEs [10,30,31].

4. Conclusions

In summary, it was shown that the use of bipolar electrochemistry enables the anodization of Ti and TiAlV spheres using glycerol-based electrolytes. As a result of applying a square wave potential of ±60 V and ±65 V, TNT layers were observed on the whole surface of Ti and TiAlV spheres. The TNT layer's dimensions varied along the Ti and TiAlV spheres with the smallest inner diameter at the top of the spheres. The inner diameters of the TNTs were correlated with the inner diameter obtained for foils using a conventional anodization approach which helps to estimate the effective applied potential of the spheres during the bipolar anodization.

CRediT authorship contribution statement

Marcela Sepúlveda: Writing – review & editing, Writing – original draft, Methodology, Investigation, Data curation, Conceptualization. **Hanna Sopha:** Writing – original draft, Methodology, Investigation, Conceptualization. **Veronika Cicmancova:** Writing – review & editing, Investigation, Data curation. **Ludek Hromadko:** Writing – review & editing, Visualization, Investigation. **Jan M. Macak:** Conceptualization, Funding acquisition, Writing – review & editing.

Declaration of competing interest

The authors declare that they have no known competing financial interests or personal relationships that could have appeared to influence the work reported in this paper.

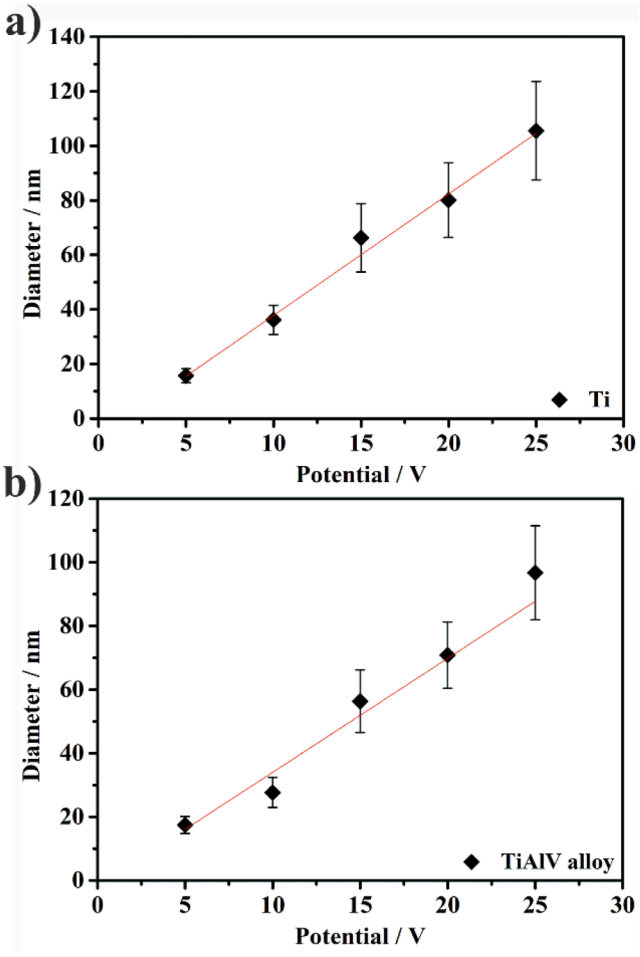

Fig. 4. Dependence of the inner TNT diameter versus the anodization potential applied on (a) Ti and (b) TiAlV foils for the conventional (non-bipolar) anodization.

Acknowledgments

The financial support from the Czech Science Foundation (project nr. 23-06793S) and the Ministry of Education, Youth and Sports of the Czech Republic for the CEMNAT large research infrastructure (project nr. LM2023037) is gratefully acknowledged.

Appendix A. Supplementary data

Supplementary data to this article can be found online at https://doi.org/10.1016/j.elecom.2024.107855.

Data availability

Data will be made available on request.

References

[1] J.R. Backhurst, J.M. Coulson, F. Goodridge, R.E. Plimley, M. Fleischmann, A preliminary investigation of fluidized bed electrodes, J. Electrochem. Soc. 116 (1969) 1600.

[2] K. Wiesener, D. Ohms, G. Benczúr-Ürmössy, M. Berthold, F. Haschka, High power metal hydride bipolar battery, J. Power Sources 84 (1999) 248–258.

[3] K.G. Ellis, R.E.W. Jansson, Further studies on the epoxidation of propylene in a bipolar trickle bed, J. Appl. Electrochem. 11 (1981) 531–535.

[4] G. Loget, S. So, R. Hahn, P. Schmuki, Bipolar anodization enables the fabrication of controlled arrays of TiO 2 nanotube gradients, J. Mater. Chem. A Mater. 2 (2014) 17740–17745.

[5] G. Loget, P. Schmuki, H2 mapping on Pt-loaded TiO2 nanotube gradient arrays, Langmuir 30 (2014) 15356–15363.

[6] H. Asoh, M. Ishino, H. Hashimoto, AC-Bipolar anodization of aluminum: Effects of frequency on thickness of porous alumina films, J. Electrochem. Soc. 165 (2018) C295.

[7] H. Asoh, M. Ishino, H. Hashimoto, Indirect oxidation of aluminum under an AC electric field, RSC Adv. 6 (2016) 90318–90321.

[8] H. Asoh, F. Ishizuka, S. Kuroki, R. Takeuchi, DC bipolar anodization of aluminum: Wider anode area than expected on the bipolar electrodes, Electrochem. Commun. 125 (2021) 107015.

[9] Q. Zhang, H. Zhou, M. Yang, X. Tang, Q. Hong, Z. Yang, S. Liu, J. Chen, G. Zhou, C. Pan, Fabrication and formation mechanism of gradient TiO2 nanotubes via bipolar anodization, J. Electroanal. Chem. 915 (2022) 116337.

[10] Y. Kokubo, H. Asoh, Anodic oxidation of wireless niobium electrode in bipolar electrochemistry, J. Electroanal. Chem. 967 (2024) 118488.

[11] G. Loget, D. Zigah, L. Bouffier, N. Sojic, A. Kuhn, Bipolar electrochemistry: from materials science to motion and beyond, Acc. Chem. Res. 46 (2013) 2513–2523.

[12] R.M. Crooks, Principles of bipolar electrochemistry, ChemElectroChem 3 (2016) 357–359.

[13] S. Ono, C. Wada, H. Asoh, Structure and property of anodic barrier films formed on aluminum in low voltage range, Electrochim. Acta 50 (2005) 5103–5110.

[14] H. Asoh, R. Takeuchi, H. Hashimoto, Unusual surfaces with structural gradients: Investigation of potential gradients on bipolar electrodes during bipolar anodization of aluminum, Electrochem. Commun. 120 (2020) 106849.

[15] H. Sopha, M. Baudys, L. Hromadko, M. Lhotka, D. Pavlinak, J. Krysa, J.M. Macak, Scaling up anodic TiO2 nanotube layers–Influence of the nanotube layer thickness on the photocatalytic degradation of hexane and benzene, Appl. Mater. Today 29 (2022) 101567.

[16] H. Sopha, M. Baudys, M. Krbal, R. Zazpe, J. Prikryl, J. Krysa, J.M. Macak, Scaling up anodic TiO2 nanotube layers for gas phase photocatalysis, Electrochem. Commun. 97 (2018) 91–95.

[17] H. Sopha, A. Kashimbetova, L. Hromadko, I. Saldan, L. Celko, E.B. Montufar, J. M. Macak, Anodic TiO2 nanotubes on 3D-printed titanium meshes for photocatalytic applications, Nano Lett. 21 (2021) 8701–8706.

[18] H. Sopha, L. Hromadko, M. Motola, J.M. Macak, Fabrication of TiO2 nanotubes on Ti spheres using bipolar electrochemistry, Electrochem. Commun. 111 (2020) 106669.

[19] H. Sopha, A. Kashimbetova, M. Baudys, P.K. Chennam, M. Sepúlveda, J. Rusek, E. Kolibalova, L. Celko, E.B. Montufar, J. Krysa, Flow-through gas phase photocatalysis using TiO2 nanotubes on wirelessly anodized 3D-printed TiNb meshes, Nano Lett. 23 (2023) 6406–6413.

[20] S.E. Fosdick, K.N. Knust, K. Scida, R.M. Crooks, Bipolar electrochemistry, Angew. Chem. Int. Ed. 52 (2013) 10438–10456.

[21] C. Kumsapaya, M. Bakaï, G. Loget, B. Goudeau, C. Warakulwit, J. Limtrakul, A. Kuhn, D. Zigah, Wireless electrografting of molecular layers for Janus particle synthesis, Chem. -A Euro. J. 19 (2013).

[22] G. Loget, J. Roche, A. Kuhn, True bulk synthesis of Janus objects by bipolar electrochemistry, Adv. Mater. 37 (2012) 5111–5116.

[23] W. Wei, F. Björefors, L. Nyholm, Hybrid energy storage devices based on monolithic electrodes containing well-defined TiO2 nanotube size gradients, Electrochim. Acta 176 (2015) 1393–1402.

[24] P. Mu, Y. Li, Y. Zhang, Y. Yang, R. Hu, X. Zhao, A. Huang, R. Zhang, X. Liu, Q. Huang, High-throughput screening of rat mesenchymal stem cell behavior on gradient TiO2 nanotubes, ACS Biomater. Sci. Eng. 4 (2018) 2804–2814.

[25] J. Capek, M. Sepúlveda, J. Bacova, J. Rodriguez-Pereira, R. Zazpe, V. Cicmancova, P. Nyvltova, J. Handl, P. Knotek, K. Baishya, Ultrathin TiO2 coatings via atomic layer deposition strongly improve cellular interactions on planar and nanotubular biomedical Ti substrates, ACS Appl. Mater. Interfaces (2024).

[26] H. Sopha, L. Hromadko, K. Nechvilova, J.M. Macak, Effect of electrolyte age and potential changes on the morphology of TiO2 nanotubes, J. Electroanal. Chem. 759 (2015) 122–128.

[27] J.M. Macak, H. Hildebrand, U. Marten-Jahns, P. Schmuki, Mechanistic aspects and growth of large diameter self-organized TiO2 nanotubes, J. Electroanal. Chem. 621 (2008) 254–266.

[28] E. Matykina, A. Conde, J. De Damborenea, D.M. y Marero, M.A. Arenas, Growth of TiO2-based nanotubes on Ti–6Al–4V alloy, Electrochim. Acta 56 (2011) 9209–9218.

[29] J.M. Macak, H. Tsuchiya, L. Taveira, A. Ghicov, P. Schmuki, Self-organized nanotubular oxide layers on Ti-6Al-7Nb and Ti-6Al-4V formed by anodization in NH4F solutions, J. Biomed. Mater. Res. A 75 (2005) 928–933.

[30] R. Takeuchi, H. Asoh, Effects of size and position of an unconnected aluminum electrode on bipolar anodization in an AC electric field, Sci. Rep. 11 (2021) 22496.

[31] Y. Kokubo, H. Asoh, Detection of the oxidation area by spectrophotometry: regional and temporal changes in anodic oxidation on titanium in bipolar electrochemistry, ACS Omega 8 (2023) 27024–27029.